

## Further Aspects of the Reaction $\pi^-p \rightarrow \pi^- \pi^+ n$ at 8 GeV/c

K. Takahashi,\* T. Sato,\* T. Kitagaki, S. Tanaka, K. Abe,  
K. Hasegawa, M. Kondo, R. Sugahara, K. Tamai,  
H. Kichimi, T. Okusawa, and S. Nugochi  
*Department of Physics, Tohoku University, Sendai, Japan*

and

S. J. Barish and W. Selove  
*Department of Physics, University of Pennsylvania, † Philadelphia, Pennsylvania 19104*

and

J. A. Poirier and N. N. Biswas  
*Department of Physics, University of Notre Dame, ‡ Notre Dame, Indiana 46556*

and

H. Yuta  
*Argonne National Laboratory, † Argonne, Illinois 60439*  
(Received 4 May 1972)

A sample of 3567 events of the reaction  $\pi^-p \rightarrow \pi^- \pi^+ n$  was obtained from the measurement of about 50 600 two-prong events in an exposure of the Brookhaven National Laboratory 80-in. hydrogen bubble chamber to an 8-GeV/c  $\pi^-$  beam. The production and decay angular distributions for the  $\rho^0$  were studied comparing with the predictions of the absorptive one-pion-exchange and vector-dominance models. The production and decay angular distributions of the  $f^0$  were also analyzed and compared with the prediction of the gauge-invariance model. A study of the  $\pi^+ \pi^-$  mass distribution suggests an enhancement at  $\sim 2100$  MeV.

### I. INTRODUCTION

The single-pion production process has long been of interest for the study of  $\pi\pi$  scattering and resonances; and more recently the details of  $\rho^0$  production and decay have taken on particular interest in connection with tests of the vector-dominance model (VDM). A number of recent theoretical papers<sup>1-5</sup> have brought forward refined treatments of one-pion-exchange models and of VDM. Some of these works emphasize the importance of data at very small  $|t|$  (invariant four-momentum transfer squared).

In this report, we present an analysis of 3567 events of the reaction

$$\pi^-p \rightarrow \pi^- \pi^+ n \quad (1)$$

in 8-GeV/c  $\pi^-p$  interactions. These data were obtained in three separate measurements done at the University of Notre Dame, the University of Pennsylvania, and Tohoku University. In this report, we treat a data sample 50% larger than that used in a previous report on this experiment,<sup>6</sup> and we have carried out some additional kinds of analysis. Topics of particular interest include a comparison of the details of  $\rho^0$  production and decay with par-

ticular reference to the behavior at small  $|t|$ , and with a view to making comparisons with the absorptive one-pion-exchange model (OPEA) and the VDM. We have also examined  $f^0$  production and decay, and compared with a gauge-invariance model; and finally, we have reexamined effects in the  $\pi\pi$  system corresponding to higher-mass resonances.

### II. EXPERIMENTAL PROCEDURE

The data reported here were all obtained from exposures in the Brookhaven National Laboratory 80-in. hydrogen bubble chamber. The Notre Dame group measured 50 000 pictures with an 8-GeV/c  $\pi^-$  beam. The Pennsylvania group and the Tohoku group shared an exposure of 100 000 pictures obtained by the Pennsylvania group with a 7.9-GeV/c  $\pi^-$  beam. The measurements carried out by Notre Dame and Pennsylvania have been published previously.<sup>6</sup> The Tohoku group completed the two-prong event measurement of the Pennsylvania exposure.

In total approximately 50 600 two-prong events have been measured and analyzed by the three groups. From these analyses, we have identified 3567 events of reaction (1).

At Tohoku University, 17 500 two-prong events which satisfied various criteria for measurement have been measured on a film-plane digitizer and image-plane digitizers. The missing-mass-squared distribution for  $\pi^-p \rightarrow \pi^- \pi^+ (M_m)$  was studied<sup>7</sup> to estimate the cross section for reaction (1). The total cross section for all  $\pi^-p$  interactions at 8 GeV/c was obtained by considering the pion path length, the density of the expanded hydrogen, the number of events of all topologies, and the number of incident pions, and was determined to be  $26.6 \pm 1.4$  mb. This value was multiplied by the ratio of the number of events of reaction (1) to the number of events of all topologies, and the cross section of reaction (1) was determined to be  $1.04 \pm 0.15$  mb. At Notre Dame, the cross section was obtained with similar considerations as described in detail in Ref. 6. The total cross section obtained was  $28.4 \pm 1.7$  mb, and the cross section for reaction (1) was determined to be  $0.87 \pm 0.05$  mb. At Pennsylvania, the two-prong cross section was obtained by starting with the counter value for the total cross section and multiplying the ratio of observed two-prong events to events of all topologies. After some corrections for unseen elastic events, the cross section of reaction (1) was determined to be  $0.96 \pm 0.07$  mb. These three values are in close agreement with each other. The weighted average of these three values was used to calculate the partial cross section for production of resonances. Table I summarizes these values.

At Tohoku University, 1119 events of reaction (1) were identified using the programs THRESH and GRIND from the measurement of about 17 500 two-prong events. In the University of Notre Dame experiment, about 20 500 two-prong events have been measured and 1321 events were identified as reaction (1) on the basis of HGEOM-GRIND fits. In the University of Pennsylvania experiment, about 12 600 two-prong events have been measured and 1127 events were identified as reaction (1) on the basis of TRED-KICK fits. The selection criteria for reaction (1) used by the three groups were similar and can be summarized as follows:

- (a) There is no elastic fit.
  - (b) Ionization of the positive particle is consistent with the fitted momentum.
  - (c) Probability for reaction (1) is greater than 1% (Notre Dame), 5% (Pennsylvania and Tohoku).
  - (d) The square of the missing mass is in the interval from 0.30 to 1.50 GeV<sup>2</sup> (Notre Dame) and from 0.30 to 1.44 GeV<sup>2</sup> (Pennsylvania and Tohoku).
- It is estimated that there was about 10% contamination from misclassified events and about 10% loss from events misclassified into other multi-neutral events. Contamination due to high-momentum-proton events was estimated to be less than a few percent.

### III. GENERAL CHARACTERISTICS OF THE REACTION

Figure 1 shows the  $\pi^+ \pi^-$  invariant-mass spectrum for reaction (1). Figure 1(b) is the Tohoku data, Fig. 1(c) is the Notre Dame data, Fig. 1(d) is the Pennsylvania data, and Fig. 1(a) is the combined data. As clearly seen, the  $\rho^0$  and  $f^0$  mesons are prominent. About 24% of all events correspond to  $\rho^0$  production and about 17% to  $f^0$  production.

The  $g^0$  meson with a peak mass value of 1670 MeV is also observed. In addition, a bump is seen at a mass of 2070 MeV peaking about 3 standard deviations above background. We have fitted the distribution with a smooth nonresonant background plus four resonances of Breit-Wigner type and have obtained the resonance parameters given in Table II.

In order to see the possible kinematical reflection on the  $\pi^+ \pi^-$  mass distribution from nucleon isobar production, we have shown, in Fig. 2, the scatter plot of the  $\pi^+ \pi^-$  invariant mass versus the  $\pi^+ n$  invariant mass with a histogram projected on each invariant mass axis. The  $\rho^0$  and the  $f^0$  can be seen as prominent vertical bands at masses of 0.75 and 1.25 GeV, and a weaker band is seen at 1.65 GeV. The effects of possible nuclear isobars on the  $\pi^+ \pi^-$  spectrum seem to be negligible. Figure 3 shows the scatter plot of  $\cos\theta$  versus the

TABLE I. Cross sections and numbers of events for the reaction  $\pi^-p \rightarrow \pi^- \pi^+ n$  at 8 GeV/c.

Group	Beam momentum (GeV/c)	Event number	Cross section (mb)
Tohoku	7.92	1119	$1.04 \pm 0.15$
Notre Dame	8.05	1321	$0.87 \pm 0.05$
Pennsylvania	7.92	1127	$0.96 \pm 0.07$
Total event number		3567	
Weighted average cross section (mb)			$0.95 \pm 0.06$

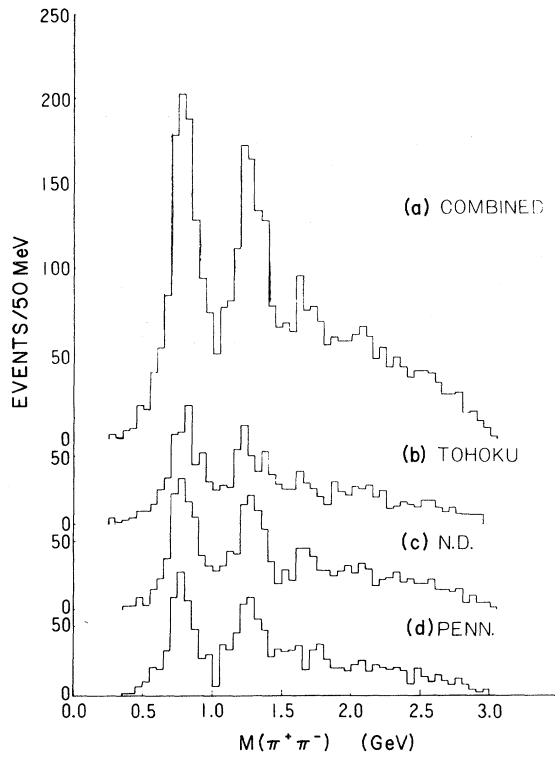


FIG. 1.  $\pi^+\pi^-$  invariant-mass distribution (a) for combined data, 3567 events, (b) for the Tohoku data, 1119 events, (c) for the Notre Dame data, 1321 events, (d) for the Pennsylvania data, 1127 events.

$\pi^+\pi^-$  invariant mass, where  $\theta$  is the angle between the direction opposite to the outgoing neutron and the outgoing  $\pi^-$  in the dipion rest frame (helicity frame). In the  $\rho^0$  and  $f^0$  bands, strong peaks are seen for "backward" angles as well as for forward angles. In the region of high  $\pi^+\pi^-$  mass, there is a strong tendency toward peripheral production, suggesting that diffractive  $\pi^+\pi^-$  scattering dominates in this region. We also note that this effect could account for the broad enhancement observed at low masses in the  $n\pi^+$  system (see Fig. 2).

#### IV. THE REACTION $\pi^-p \rightarrow \rho^0 n$

In Fig. 4 we give the production angular distribution of the  $\rho^0$ . The  $\rho^0$  mass interval was taken from 675 to 875 MeV. Non- $\rho^0$  background events

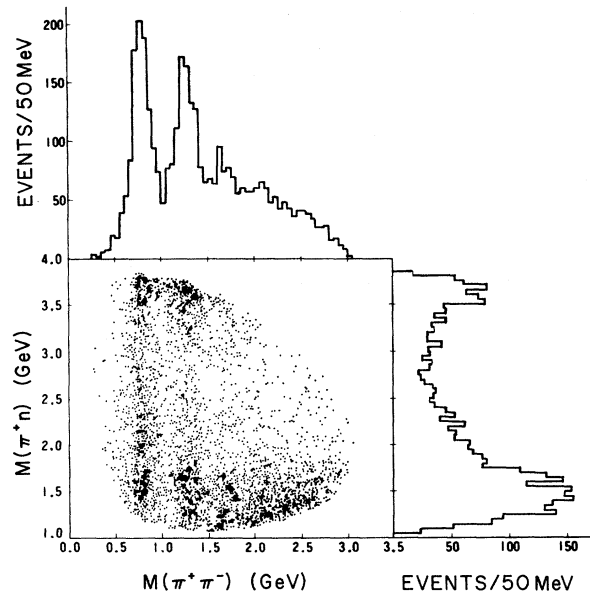


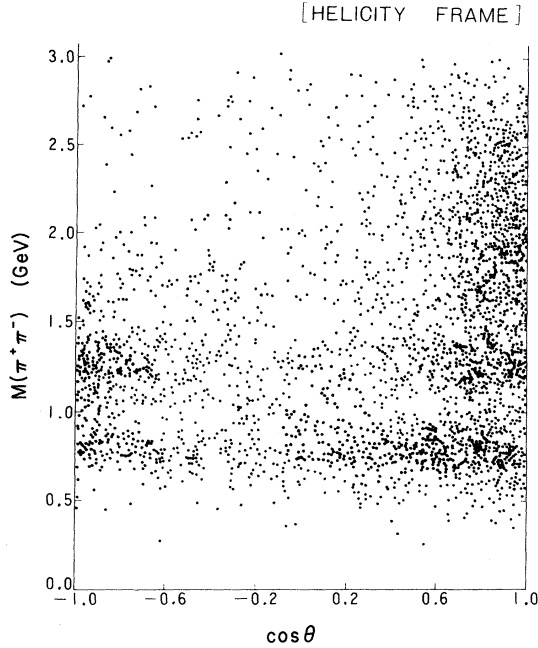
FIG. 2. Scatter plot of  $M(\pi^+\pi^-)$  versus  $M(\pi^+n)$  with the projections on both axes.

in this mass region were estimated to be about 20%. The absolute scale has been normalized to our value of the total cross section for  $\rho^0$  production shown in Table I. The resolution in  $|t|$  is estimated to be  $\sim 0.1\mu^2$  at the lower kinematic cutoff of  $|t|$  and  $\sim 0.3\mu^2$  at  $|t| \sim \mu^2$ , where  $\mu$  is the charged-pion mass. The dashed curve shown in Fig. 4 is a prediction of the one-pion-exchange model with absorption (OPEA) of Williams<sup>2</sup> and gives a reasonable description of the experimental  $d\sigma/dt$ . For comparison, the prediction of the pure one-pion-exchange model (OPE)<sup>8</sup> is also shown as the solid curve in this figure; this prediction is not in good agreement with the data.

The behavior of the differential cross section  $d\sigma/dt$  is of particular interest. In an earlier report on two-thirds of the present data, it was observed that  $d\sigma/dt$  showed no dip at the smallest values of  $|t|$ .<sup>9</sup> With the addition of data included in the present report, we see that this is still true. We note that a recent experiment at 15 GeV/c, with much higher statistics than ours, shows that  $d\sigma/dt$  for  $\rho^0$  production does fall at the smallest  $|t|$  values.<sup>10</sup> The data in Fig. 4 disagree

TABLE II. Resonance parameters for the combined data.

Resonance	Cross section (mb)	Mass (GeV)	Width (GeV)
$\rho^0 \rightarrow \pi^+\pi^-$	$0.233 \pm 0.018$	$0.787 \pm 0.010$	$0.144 \pm 0.012$
$f^0 \rightarrow$	$0.169 \pm 0.014$	$1.258 \pm 0.010$	$0.166 \pm 0.014$
$g^0 \rightarrow$	$\sim 0.04$	$\sim 1.67$	$\sim 0.18$
$g^0(2070) \rightarrow \pi^+\pi^-$	$\sim 0.02$	$\sim 2.07$	$\sim 0.16$

FIG. 3. Scatter plot of  $\cos\theta$  versus  $M(\pi^+\pi^-)$ .

with the behavior of the data in Ref. 10, but only by 2 standard deviations in the first bin.

We have analyzed the decay angular distribution of the events in the  $\rho^0$  mass band. In our analysis, we have utilized the decay variables,  $\cos\theta$  and  $\phi$ , in the helicity frame as well as in the Gottfried-Jackson frame. Between these two reference frames, the choice of the spin quantization axis ( $z$  axis) differs: In the helicity frame, the  $z$  axis is opposite to the direction of the outgoing neutron in the  $\rho^0$  rest system, whereas in the Gottfried-Jackson frame, it is chosen as the direction of the incident pion. Figure 5 shows the scatter plot

$$W(\theta, \phi) = \frac{3}{4\pi} [\rho_{00} \cos^2\theta + \rho_{11} \sin^2\theta - \sqrt{2} \operatorname{Re}(\rho_{10}) \sin 2\theta \cos\phi - \rho_{1-1} \sin^2\theta \cos 2\phi] \\ + \frac{\sqrt{3}}{4\pi} [-2\sqrt{2} \operatorname{Re}(\rho_{10}^{SP}) \sin\theta \cos\phi + 2 \operatorname{Re}(\rho_{00}^{SP}) \cos\theta] + \frac{1}{4\pi} \rho_{00}^S, \quad (2)$$

where  $\rho_{00}^S$  corresponds to pure  $S$ -wave effects and  $\rho_{00}^{SP}$  and  $\rho_{10}^{SP}$  correspond to  $S$ - $P$  interference effects. Normalization was made according to the equation

$$\rho_{00} + 2\rho_{11} + \rho_{00}^S = 1. \quad (3)$$

The explicit dependence of Eq. (2) on  $\rho_{00}^S$  may be eliminated and the relevant quantities which may be determined experimentally are  $(\rho_{00} - \rho_{11})$ ,  $\operatorname{Re}(\rho_{10})$ ,  $\rho_{1-1}$ ,  $\operatorname{Re}(\rho_{10}^{SP})$ , and  $\operatorname{Re}(\rho_{00}^{SP})$ . We have obtained the values of these elements from the observed decay angular distributions by the least-squares method. The density-matrix elements thus obtained in the helicity frame are shown in

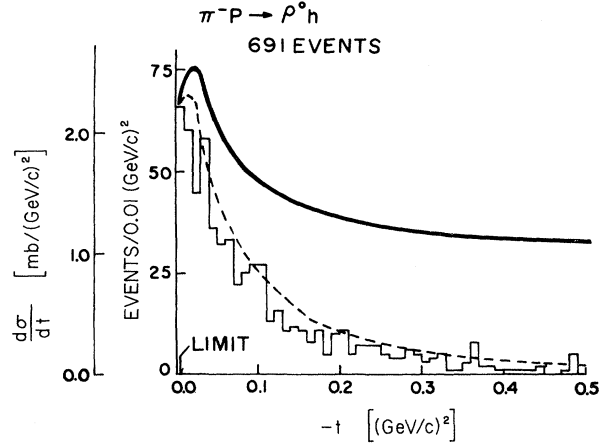


FIG. 4. Differential cross section  $d\sigma/dt$  for the  $\rho^0$  mass region, 675 to 875 MeV. The solid curve is the prediction of the pure one-pion-exchange model and the dashed curve is the prediction of one-pion exchange with absorption corrections. No correction has been made for the kinematic cutoff in the first bin.

of  $\cos\theta$  versus  $\phi$  in the helicity frame together with the projections on both axes. A strong diagonal correlation between  $\cos\theta$  and  $\phi$  is seen as was observed previously.<sup>6</sup> The asymmetry parameter in  $\cos\theta$ ,  $R = (F - B)/(F + B)$ , is found to be  $0.35 \pm 0.04$  in the helicity frame, where  $F$  and  $B$  are the number of events with  $\cos\theta \geq 0$  and  $\cos\theta < 0$ , respectively. The forward-backward asymmetry found here corresponds to the long-known presence of a substantial  $S$ -wave  $\pi^+\pi^-$  interaction in the  $\rho^0$  mass region.

If both  $S$ - and  $P$ -wave pion-pion interactions are considered, the general decay angular distribution can be expressed with the density-matrix elements  $\rho_{mm'}$  in an appropriate frame, and it is expressed as follows:

Fig. 6. The solid curves in Fig. 6 are the theoretical calculations in the OPEA model<sup>2</sup> neglecting any  $S$ -wave contributions. Here again, the OPEA predictions are in reasonable agreement with the data.

We compared the density-matrix elements with those obtained from the 15-GeV/c  $\pi^-p$  data of Bulos *et al.*<sup>10</sup> and found that  $\rho_{00} - \rho_{11}$ ,  $\operatorname{Re}(\rho_{00}^{SP})$ , and  $\operatorname{Re}(\rho_{10}^{SP})$  are in reasonable agreement with each other. However, our  $\rho_{1-1}$  seems to show a negative value for  $t$  between  $-0.1$  and  $-0.4$  GeV<sup>2</sup>, whereas  $\rho_{1-1}$  in Ref. 10 shows a positive value for this  $t$  range. We also note that  $\rho_{1-1}$  obtained from the

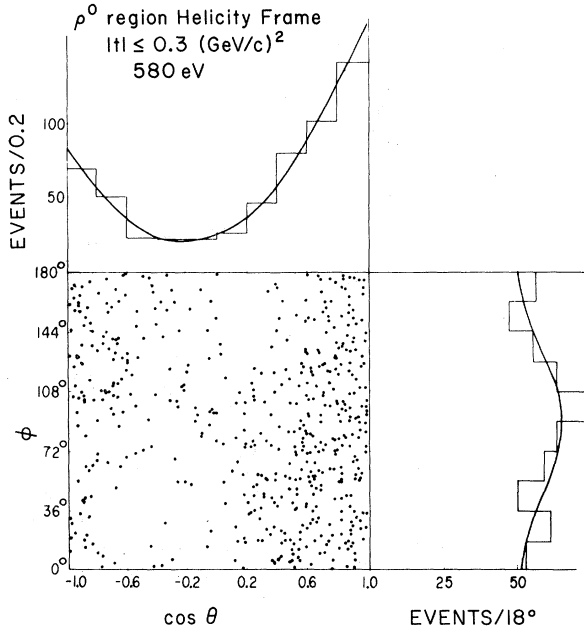


FIG. 5. Scatter plot of  $\cos\theta$  versus  $\phi$  with the projections on both axes for the  $\rho^0$  events with  $|t| \leq 0.3 \text{ (GeV/c)}^2$ . The solid curves are fits with expression (2).

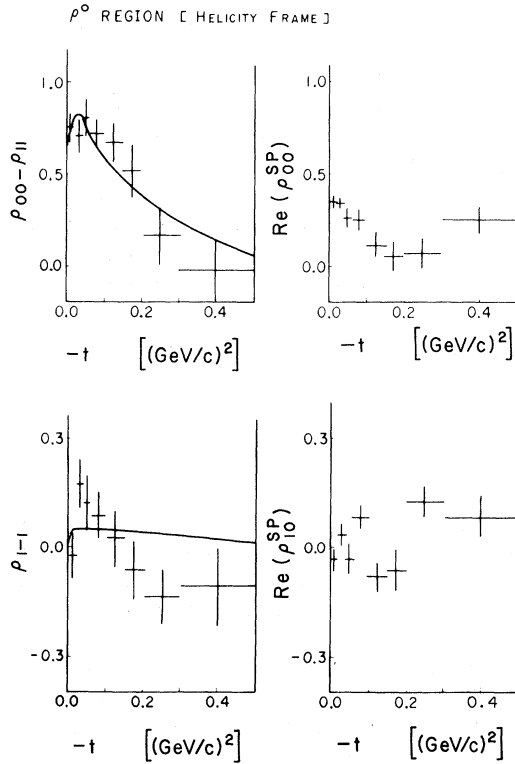


FIG. 6. Density-matrix elements for the  $\rho^0$  as a function of  $t$  in the helicity frame. Theoretical curves are predictions of one-pion exchange with absorption corrections.

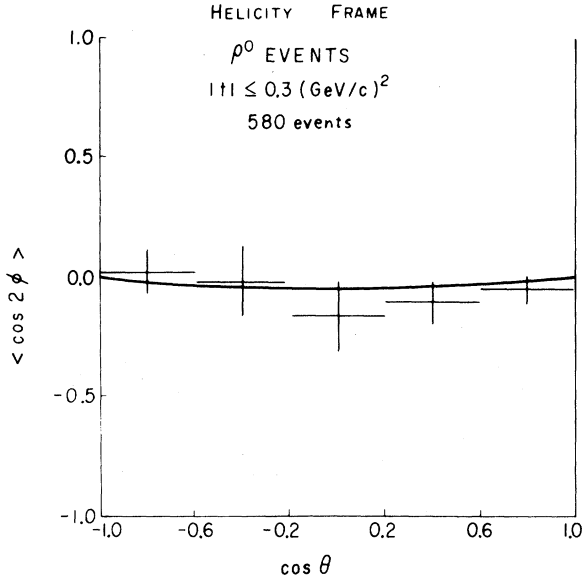


FIG. 7. Distribution of  $\langle \cos 2\phi \rangle$  versus  $\cos\theta$  for the  $\rho^0$  events with  $|t| \leq 0.3 \text{ (GeV/c)}^2$ . The solid curve is a fit with expression (4).

4-GeV/c  $\pi^-p$  bubble-chamber data of Johnson *et al.*<sup>11</sup> shows a negative value for this  $t$  range.

It was suggested by Gell-Mann and Zachariassen<sup>12</sup> that the hadronic electromagnetic currents are dominated by the vector mesons  $\rho$ ,  $\omega$ , and  $\phi$ . Various theoretical predictions and their experimental tests have been carried out.<sup>4, 10</sup> Recently Biswas *et al.*<sup>13</sup> discussed the effect of some possible  $D$ -wave  $\pi\pi$  interaction in the  $\rho^0$  mass region in connection with the validity of the vector-dominance model. We checked for the presence of  $D$ -wave effects in the  $\rho^0$ -mass region in the same manner as Biswas *et al.* before we tested the vector-dominance prediction. For a  $P$ -wave interaction, it can be shown that the average value of the quantity  $\cos 2\phi$  as a function of  $\theta$  is given by

$$\langle \cos 2\phi \rangle = \frac{3}{4} \rho_{1-1} \sin^2 \theta, \quad (4)$$

and it is independent of the presence or absence of  $S$ -wave  $\pi\pi$  interaction; but Eq. (4) is no longer valid if partial waves with  $l \geq 2$  are taken into account. Figure 7 shows the values of  $\langle \cos 2\phi \rangle$  as a function of  $\cos\theta$  for the  $\rho^0$  events with  $|t| \leq 0.3 \text{ (GeV/c)}^2$  in the helicity frame. The solid line in the figure is the best fit with expression (4). The data seem to be in good agreement with expression (4), and  $D$ -wave effects might be negligible in the  $\rho^0$  mass region. Figure 8 shows the comparison of our measured differential cross section with the new vector-dominance predictions by Cho and Sakurai.<sup>5</sup> Figure 8(a) shows  $S^2 d\sigma/dt$ , and Fig. 8(b) shows  $2S^2 \rho_{11} d\sigma/dt$ , where  $\rho_{11}$  was calculated from the value  $(\rho_{00} - \rho_{11})$ , assuming that the  $S$ -wave contribu-

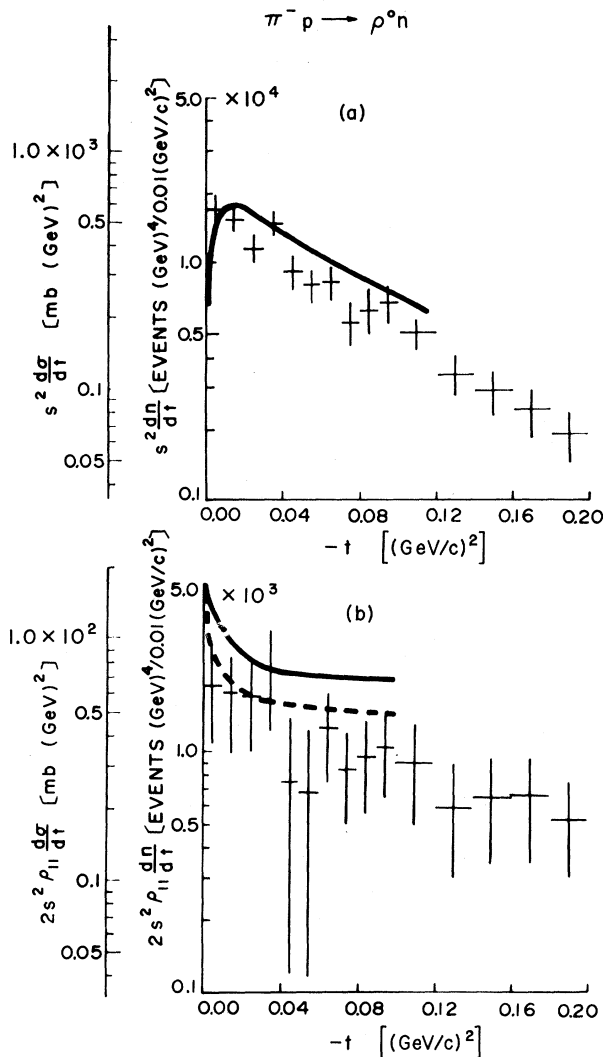


FIG. 8. The total and transverse differential cross sections as a function of momentum transfer for the  $\rho^0$ . The solid curves are the predictions of the vector-dominance model by Cho and Sakurai. The dashed curve in (b) is calculated including the 7% S-wave admixture.

tion is 7% in the  $\rho^0$  mass region.<sup>14</sup> Solid curves in the figures are taken from Cho and Sakurai.<sup>5</sup> The dashed curve in Fig. 8(b) is calculated including the 7% S-wave contribution. Figure 9 shows relevant density-matrix elements in the Gottfried-Jackson frame. The dashed curves represent the predictions by Cho and Sakurai.<sup>5</sup> Considering the fact that the theoretical curve has no variable parameter in the predictions, the agreement with the data is quite good.

#### V. THE REACTION $\pi^- p \rightarrow f^0 n$

Figure 10 shows the  $t$  distribution of the  $f^0$  cross section. The mass interval of the  $f^0$  events was taken from 1170 to 1370 MeV. The absolute scale

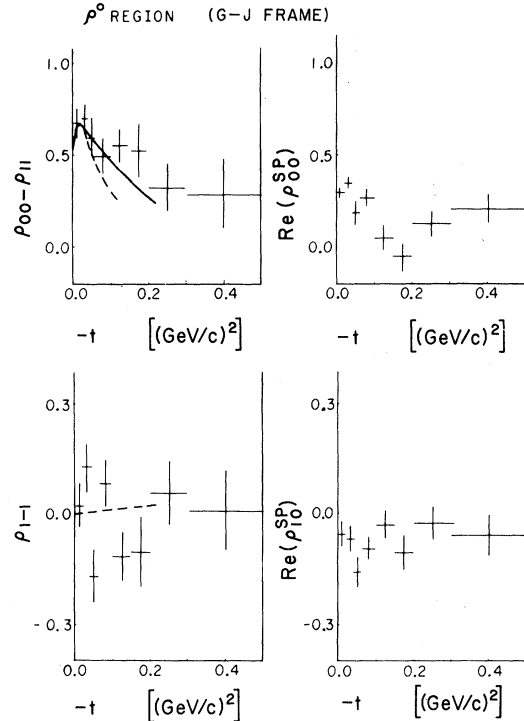


FIG. 9. Density-matrix elements for the  $\rho^0$  events in the Gottfried-Jackson frame compared with the predictions by OPEA (solid curve) and by Cho and Sakurai (dashed curve).

of the cross section has been normalized to our estimate of the production cross section of the  $f^0$  given in Table II. The first bin in Fig. 10 has been corrected for the kinematical limit of  $t$ .

Hogaasen *et al.*<sup>15</sup> have calculated the production and decay angular distributions for the  $f^0$  using the OPEA model and have obtained the results that the OPEA prediction of the cross section is larger than the experimental value by a factor of about 2. Poirier *et al.*<sup>6</sup> have also compared the predictions with the 8-GeV/c  $\pi^-$  data and found the same results. In this paper, instead of showing the OPEA predictions, we will compare the data with predictions of Takeda *et al.*<sup>16</sup> This calculation is based on gauge invariance in analogy to the vector-dominance model for the  $\rho^0$  case and no absorption effects are included. The dashed curve in Fig. 10 is the predicted shape from this model. For comparison, we also show the OPE prediction<sup>15</sup> as the solid curve. Both curves are normalized to the experimental  $d\sigma/dt$  at  $t = -0.02$   $(\text{GeV}/c)^2$ ; the normalization factors are 2.5 for the gauge invariance model and 2.4 for OPE. We note that the predicted shape of the gauge-invariance model gives better agreement with the data than that of OPE.

The decay angular distributions of the  $f^0$  events have also been analyzed. As in the  $\rho^0$  case, the

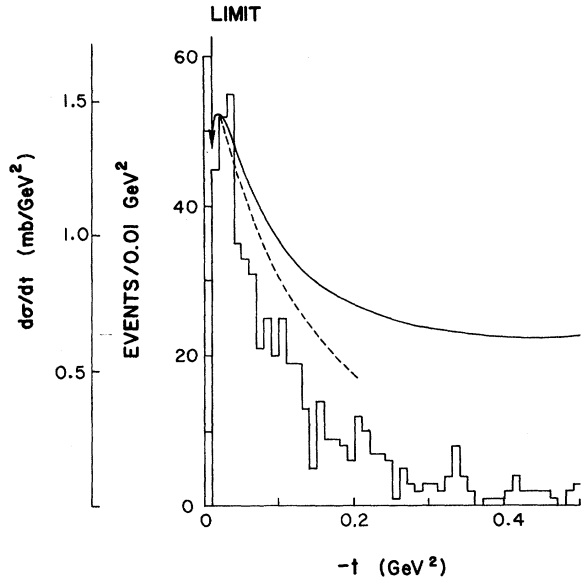


FIG. 10. Differential cross section  $d\sigma/dt$  for the  $f^0$  mass region, 1170 to 1370 MeV. The solid and dashed curves are the predictions of pure one-pion exchange and the gauge-invariance model, respectively.

decay angles  $\theta$  and  $\phi$  have been evaluated in the helicity frame. Figure 11 shows the scatter plot of  $\cos\theta$  versus  $\phi$  in the helicity frame together with the projections on both axes. A fairly strong diagonal correlation is also seen here, as in the  $\rho^0$  case. It is interesting to note that the  $\cos\theta$  distribution is more symmetric than in the case of the  $\rho^0$ , but the  $\phi$  distribution looks less symmetric.

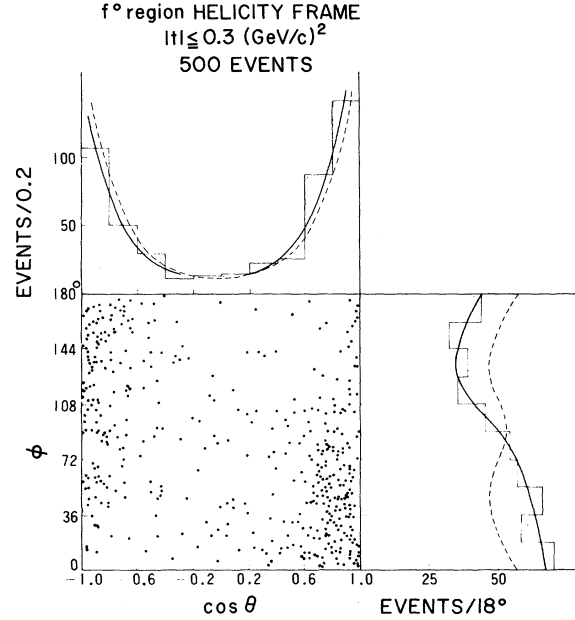


FIG. 11. Scatter plot of  $\cos\theta$  versus  $\phi$  with the projections on both axes for the  $f^0$  events with  $|t| \leq 0.3$   $(\text{GeV}/c)^2$ . The dashed curves are fits using pure  $D$  wave according to expression (5); the solid curve uses both  $P$  and  $D$  waves.

This seems to indicate that there might be non- $D$ -wave background in the  $f^0$  mass region. Considering only the  $D$ -wave component for the  $f^0$ , the decay angular distribution can be expressed in terms of the density-matrix elements  $\rho_{mm'}$ , in an appropriate frame, and is given by

$$\begin{aligned}
 W(\theta, \phi) = & \left( \frac{15}{16\pi} \right) \{ \sin^4\theta(\rho_{22} + \rho_{2-2} \cos 4\phi) + \sin^2 2\theta(\rho_{11} - \rho_{1-1} \cos 2\phi) + 3\rho_{00}(\cos^2\theta - \frac{1}{3})^2 \\
 & - 4 \sin^3\theta \cos\theta [\text{Re}(\rho_{21}) \cos\phi - \text{Re}(\rho_{2-1}) \cos 3\phi] \\
 & + (2\sqrt{6}) \text{Re}(\rho_{20}) \sin^2\theta(\cos^2\theta - \frac{1}{3}) \cos 2\phi - (2\sqrt{6}) \text{Re}(\rho_{10}) \sin 2\theta(\cos^2\theta - \frac{1}{3}) \cos\phi \}, \quad (5)
 \end{aligned}$$

where we have the normalization condition

$$\rho_{00} + 2\rho_{11} + 2\rho_{22} = 1. \quad (6)$$

The dashed curves in Fig. 11 show the results of fits for the projections on the  $\cos\theta$  and  $\phi$  axes using Eq. (5). We also fit the projections using the  $P$ - and  $D$ -wave parametrization.<sup>17</sup> The solid curves are obtained from this fit and give better agreement with the data.

Figure 12 shows some spin density-matrix elements obtained from our decay angular distributions by a least-squares fit.  $\rho_{00}$ ,  $\rho_{11}$ , and  $\rho_{22}$  were obtained by fitting Eq. (5) integrated over  $\phi$ .  $\rho_{1-1} + \sqrt{6}/3(\text{Re}\rho_{10})$  and  $\rho_{2-2}$  were obtained by fitting Eq. (5) integrated over  $\cos\theta$ . The negative  $\rho_{22}$  is due

to the background component in the  $f^0$  mass region. Solid curves in these figures are the theoretical predictions of the gauge-invariance model. This model describes the experimental  $\rho_{00}$  fairly well, but not other density-matrix elements. It is, however, interesting to note that this gauge-invariance model predicts nonzero values for  $\rho_{11}$ ,  $\rho_{1-1}$ , and  $\text{Re}(\rho_{20})$  without inclusion of absorption effects.

Since there exists a large amount of non- $D$ -wave background in the  $f^0$  mass region,<sup>17</sup> the density-matrix elements assuming a pure  $D$  wave for the  $f^0$  represent too simple an analysis and should not be taken as correct. A recent paper by Carroll *et al.*<sup>18</sup> gives a detailed analysis of the  $f^0$  region using a considerable amount of data at 7 GeV/c.

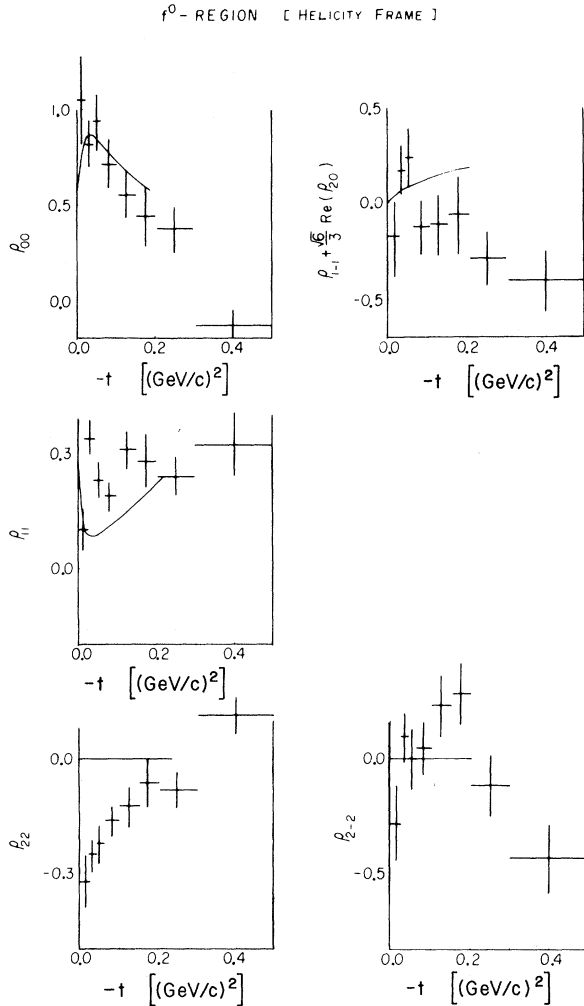


FIG. 12. The  $f^0$  density-matrix elements in the helicity frame as a function of  $t$ . Theoretical curves are predictions of the gauge-invariance model.

## VI. SEARCH FOR A POSSIBLE DIPION RESONANCE

As shown in Fig. 1(a), together with the  $\rho^0$  and the  $f^0$ , the  $g^0$  peak at 1670 MeV can be seen. To investigate possible dipion effects in the high  $\pi\pi$  mass region, Fig. 13 shows the  $\pi^+\pi^-$  mass distribution with 75 MeV mass bins. Above the  $g^0$ , we observe a possible effect at about 2070 MeV which is about 3 standard deviations above background. We have also plotted the dipion mass spectra for the events in the backward region of  $\cos\theta$  where we expect to have less background. Figure 14(a) is for the events with  $\cos\theta \leq -0.5$  and Fig. 14(b) is for those with  $\cos\theta \leq -0.8$ . These distributions, however, do not show any statistically significant peak at 2070 MeV.

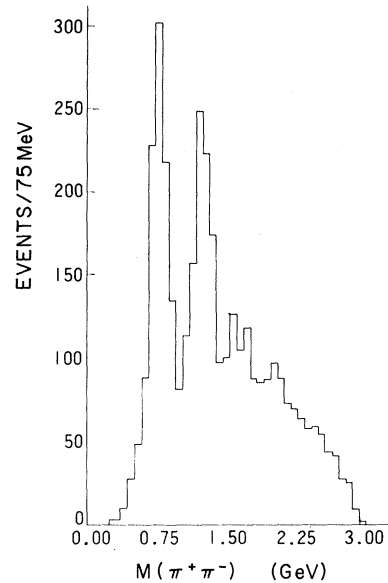


FIG. 13.  $\pi^+\pi^-$  invariant-mass distribution for combined data, 3567 events with 75-MeV mass bins.

The decay angular distribution of the  $\pi^+\pi^-$  system is analyzed as a function of dipion mass in the helicity frame, giving various moments for Legendre polynomials. The  $\langle P_l \rangle$  moments ( $l=1$  to 8) are shown in Fig. 15. Again, no significant effects were observed in these distributions near 2100 MeV.

Several experiments have been carried out to search for high-mass dipion resonances and some evidence for resonances at about 2100 MeV has been reported.<sup>19</sup> The effect observed at 2080 MeV in our data may correspond to the effect reported in those experiments.

## VII. CONCLUSIONS

We have studied the reaction  $\pi^-p \rightarrow \pi^- \pi^+ n$  at 8 GeV/c, and have observed the production of  $\rho^0$ ,  $f^0$ , and  $g^0$  mesons. An indication of a new resonance at a  $\pi^+\pi^-$  mass of 2070 MeV is also seen. The  $\pi^+n$  invariant mass distribution indicates that isobar production is relatively small, and that the effects on the  $\pi^+\pi^-$  mass distribution from isobar reflection are weak. The production and the decay angular distributions for the  $\rho^0$  have been studied and the density-matrix elements have been calculated assuming an S-wave  $\pi^+\pi^-$  interaction is present together with the P wave. These data have been analyzed in terms of the one-pion-exchange model with absorption (OPEA). It is shown that the predictions of OPEA are in good agreement with the data.

We have also compared our data on  $\rho^0$  production in the very forward region with the predictions



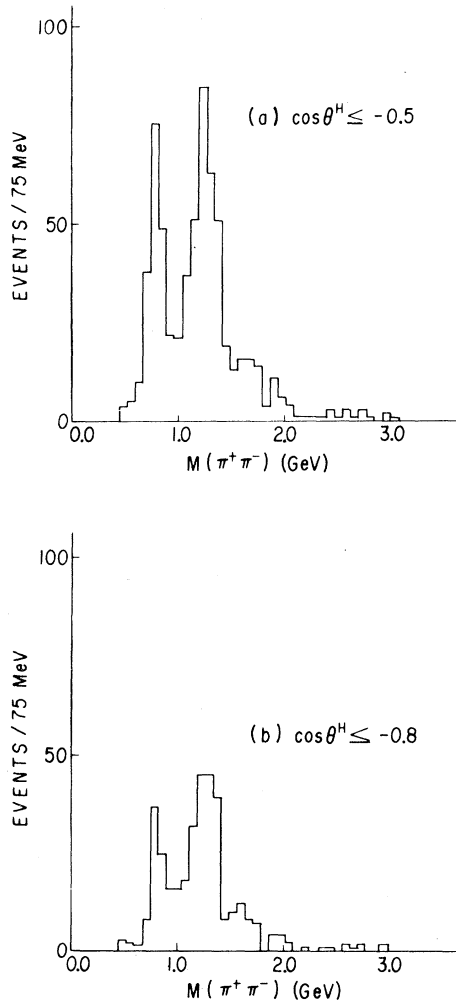


FIG. 14.  $\pi^+\pi^-$  invariant-mass distribution for the events (a) with  $\cos\theta^H \leq -0.5$  and (b)  $\cos\theta^H \leq -0.8$ .

of the vector-dominance model (VDM). The VDM predictions are in good agreement with the observed differential cross section and with the  $P$ -wave density-matrix elements.

The production and decay angular distributions have been studied in the  $f^0$  mass region. The  $\cos\theta$  distribution is more symmetric than in the case of the  $\rho^0$ , but the  $\phi$  distribution is relatively asymmetric. This might be due to the possible presence of non- $D$ -wave  $\pi^+\pi^-$  interactions in the  $f^0$  region. The gauge-invariance model without absorption effects seems to give a fairly good description of the shape of  $d\sigma/dt$  and  $\rho_{00}$  for the  $f^0$ .

The production and decay angular distributions of the  $\pi^+\pi^-$  system were studied in the vicinity of a small bump found at 2070 MeV. Weak evidence is found suggesting that this bump might correspond to a  $\pi^+\pi^-$  resonance.

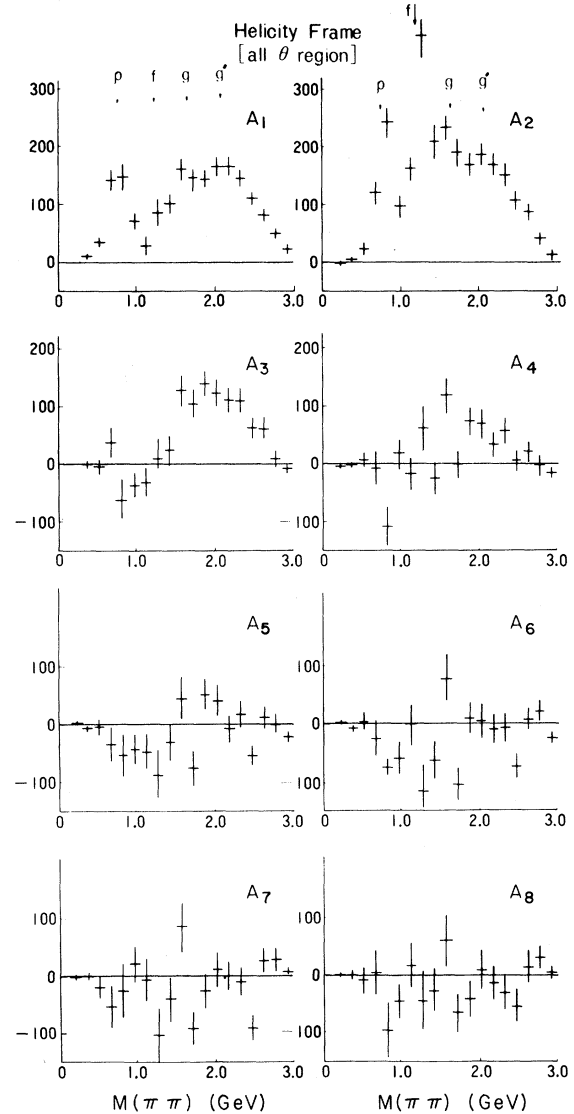


FIG. 15. Legendre polynomial coefficients as a function of  $\pi^+\pi^-$  mass.

#### ACKNOWLEDGMENTS

This work was made possible by the help and cooperation of the Shutt Bubble Chamber Group and the AGS personnel of Brookhaven National Laboratory. We wish to thank the Scanning and Measuring Staff of the Tohoku University, of the University of Pennsylvania, and of the University of Notre Dame for their assistance with the data analysis. We also thank Dr. N. M. Cason, Dr. V. P. Kenney, and Dr. W. D. Shephard for their interest in this experiment. The authors from the Tohoku group would like to thank Professor Gyo Takeda for his enlightening discussions and encouragement.

\*Present address: Physics Division, National Laboratory for High Energy Physics, Tsukuba, Ibaraki.

†Work supported in part by the U. S. Atomic Energy Commission.

‡Work supported in part by the National Science Foundation.

<sup>1</sup>F. Henyey *et al.*, Phys. Rev. **182**, 1579 (1969).

<sup>2</sup>P. K. Williams, Phys. Rev. D **1**, 1312 (1970); G. L. Kane and Marc Ross, Phys. Rev. **177**, 2353 (1969);

G. L. Kane, in *Experimental Meson Spectroscopy*, edited by C. Baltay and A. H. Rosenfeld (Columbia Univ. Press, New York, 1970).

<sup>3</sup>L. Chan, V. Hagopian, and P. K. Williams, Phys. Rev. D **2**, 583 (1970).

<sup>4</sup>J. J. Sakurai, Ann. Phys. (N.Y.) **11**, 1 (1960); C. Iso and H. Yoshii, *ibid.* **47**, 424 (1968); Y. Avni and H. Harari, Phys. Rev. Letters **23**, 262 (1969).

<sup>5</sup>C. F. Cho and J. J. Sakurai, Phys. Rev. D **2**, 517 (1970).

<sup>6</sup>J. A. Poirier *et al.*, Phys. Rev. **163**, 1462 (1967); S. J. Barish *et al.*, *ibid.* **184**, 1375 (1968).

<sup>7</sup>The Tohoku data were compared with the data previously published (Ref. 6) and checked for the resolutions of missing mass squared,  $\pi^+\pi^-$  mass, etc. Though the resolution of the Tohoku data is a little broader than that of the other two groups, the over-all features are

very similar to each other and no significant differences have been observed.

<sup>8</sup>J. D. Jackson and H. Pilkuhn, Nuovo Cimento **33**, 906 (1964).

<sup>9</sup>W. Selove, F. Forman, and H. Yuta, Phys. Rev. Letters **21**, 952 (1968).

<sup>10</sup>F. Bulos *et al.*, Phys. Rev. Letters **26**, 1453 (1971); F. Bulos *et al.*, *ibid.* **26**, 1457 (1971).

<sup>11</sup>P. B. Johnson *et al.*, Phys. Rev. **176**, 1651 (1968).

<sup>12</sup>M. Gell-Mann and F. Zachariasen, Phys. Rev. **124**, 953 (1961).

<sup>13</sup>N. N. Biswas *et al.*, Phys. Rev. D **1**, 2705 (1970).

<sup>14</sup>L. Durand and Y. T. Chiu, Phys. Rev. Letters **14**, 329 (1965); I. Derado *et al.*, *ibid.* **14**, 872 (1965).

<sup>15</sup>H. Hogaasen *et al.*, Nuovo Cimento **42**, 323 (1966).

<sup>16</sup>G. Takeda *et al.*, paper presented at the Joint Japanese-U.S. Seminar on Elementary Particle Physics with Bubble Chamber Detectors, Stanford Linear Accelerator Center, 1971 (unpublished).

<sup>17</sup>B. Y. Oh *et al.*, Phys. Rev. D **1**, 2494 (1970).

<sup>18</sup>J. T. Carroll *et al.*, Phys. Rev. Letters **28**, 318 (1972).

<sup>19</sup>H. Nicholson *et al.*, Phys. Rev. Letters **23**, 603 (1969); E. W. Anderson *et al.*, *ibid.* **22**, 1390 (1969); S. L. Kramer *et al.*, *ibid.* **25**, 396 (1970).

## Reactions $K^-p \rightarrow \Lambda\pi^0$ and $K^-p \rightarrow \bar{K}^0n$ in the Center-of-Mass Energy Range 1700–2100 MeV\*

A. J. Van Horn, R. P. Ely, and J. Louie†

*E. O. Lawrence Berkeley Laboratory, University of California, Berkeley, California 94720*

(Received 6 March 1972)

Cross sections, angular distributions, and polarizations are presented for the reactions  $K^-p \rightarrow \Lambda\pi^0$  and  $K^-p \rightarrow \bar{K}^0n$  for 19 incident beam momenta in the c.m. energy range 1709–2106 MeV. Legendre-polynomial expansion coefficients to seventh order are also given for the data. The experimental procedures and results from two exposures in the Lawrence Berkeley Laboratory 25-in. hydrogen bubble chamber are discussed.

### I. INTRODUCTION

This paper presents new data for the reactions  $K^-p \rightarrow \Lambda\pi^0$  and  $K^-p \rightarrow \bar{K}^0n$  at 19 c.m. energies between 1709 and 2106 MeV with an average of about 0.8 events/ $\mu\text{b}$  at each energy. Several earlier experimental studies of these reactions may be found in the literature.<sup>1</sup> The data of this experiment are in an intermediate energy range which is rich in *s*-channel resonant structure. In particular our data span the region around 1900 MeV where the isospin-1 partial waves are notably ambiguous.<sup>2</sup> The reaction  $K^-p \rightarrow \Lambda\pi^0$ , a formation reaction which is pure isospin-1, should be particularly revealing of this structure. Likewise, the

charge-exchange reaction  $K^-p \rightarrow \bar{K}^0n$  can be used in conjunction with the elastic scattering measurements to determine the partial waves in this energy range.

This paper presents the experimental procedures and results from two exposures in the LBL 25-in. hydrogen bubble chamber. Cross sections, angular distributions, and polarizations are presented for 19 incident beam momenta. The Legendre-polynomial expansion coefficients are also given. The data are presented in a form which can be readily adapted for analysis, either alone or in conjunction with other experimental data.

A partial-wave analysis of the first exposure is available in unpublished form in Ref. 3, and pre-